

¹ High-Pressure Chemical Looping Reforming Processes: System Analysis for Syngas Generation from Natural Gas and Reducing Tail Gases

⁴ Peter Sandvik,[‡] Mandar Kathe,[‡] William Wang, Fanhe Kong, and Liang-Shih Fan^{*ID}

⁵ William G. Lowrie Department of Chemical and Biomolecular Engineering, The Ohio State University, 151 West Woodruff Avenue,
⁶ 340 A Koffolt Laboratories, Columbus, Ohio 43210, United States

⁷  Supporting Information

ABSTRACT: Reforming technologies produce syngas that serves as an important intermediate in the production of fuels and chemicals in the chemical and petrochemical industry. Only recently has reforming technology based on the chemical looping concept been attempted. Most chemical looping studies have been performed under ambient pressure conditions, but most processes that use syngas operate at an elevated pressure. Understanding the effect that pressure has on syngas generation in a chemical looping reactor is essential to the design of the overall system. This study characterizes and compares the effect of pressures on syngas yields under various chemical looping reforming operating conditions. Specifically, in this study, an iron-based oxygen carrier is used for the chemical looping partial oxidation reaction of methane to form syngas. The equilibrium simulation is of direct relevance to process applications, as demonstrated by the methane and metal oxide co-current reactor system, where in previous studies, experimental product yields were shown to be appropriately represented by equilibrium conditions. The results of syngas generation at 1 atm are used in this study as the basis for comparison to those obtained under pressurized conditions. The isothermal syngas generation is first examined qualitatively and quantitatively for pressures ranging from 1 to 30 atm. The adiabatic syngas generation is then examined under autothermal operating conditions. The sensitivity studies are performed to describe the changes in product yields as the temperature and pressure along with steam and CO₂ inputs are varied. The results of the analysis illustrate the various competing factors that dictate the high-pressure syngas yield and purity. The study also provides insight into choice of operating conditions that enable thermodynamic syngas yields at higher pressure to be comparable to those at atmospheric pressures.

1. INTRODUCTION

With the increasing demand in global energy consumption, it is necessary to efficiently use and convert existing fossil fuel resources to value-added chemicals, such as methanol, propylene, diesel, and other liquids.^{1–2} The conventional method of producing chemicals and/or liquid fuels from fossil fuels is indirect, with the production of syngas as a first step that is both process- and energy-intensive.^{3–7} Syngas generation using chemical looping is a proposed advancement over the conventional method, achieved through process intensification by combining several unit operations. For example, when chemical looping is used to replace a conventional syngas production system, it can eliminate the need for an air separation unit that provides molecular oxygen and a pre-reformer system that reforms heavier hydrocarbons.^{8–10} Additionally, the chemical looping system when operated at 1 atm has also shown potential for reduction in natural gas consumption by ~15–20% over a conventional reforming system for producing an equivalent amount of syngas.^{8–10} In chemical looping, a metal oxide reacts with the fuel rather than molecular oxygen or air directly, as in conventional methods.^{11–14} The syngas produced in a reducer reactor is tuned in its hydrogen/carbon monoxide ratio (H₂/CO ratio) to match the necessary downstream reaction conditions, with minimal undesirable products. The reduced metal oxide is regenerated with air in a separate reactor, the combustor reactor, and circulated back to the inlet of the

reducer reactor to complete the cyclic redox cycle, eliminating any direct contact between air and fuel. Chemical looping is considered a promising alternative that can provide efficiency and cost benefits over existing process systems.^{8–12} A basic schematic of the chemical looping reforming process is shown in Figure 1. The Ohio State University (OSU) methane to syngas (MTS) process configuration uses two reactors, a co-current moving bed reactor for the fuel and a fluidized bed reactor for the air, that allows for the conversion of fuel to

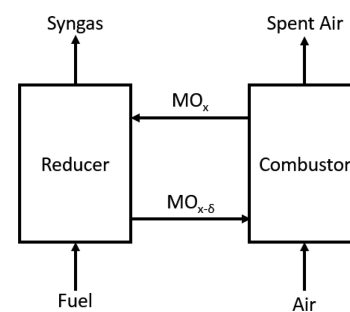


Figure 1. Basic schematic of a two-reactor chemical looping system using arbitrary metal oxide (MO) for syngas production.

Received: May 25, 2018

Revised: September 12, 2018

Published: September 14, 2018

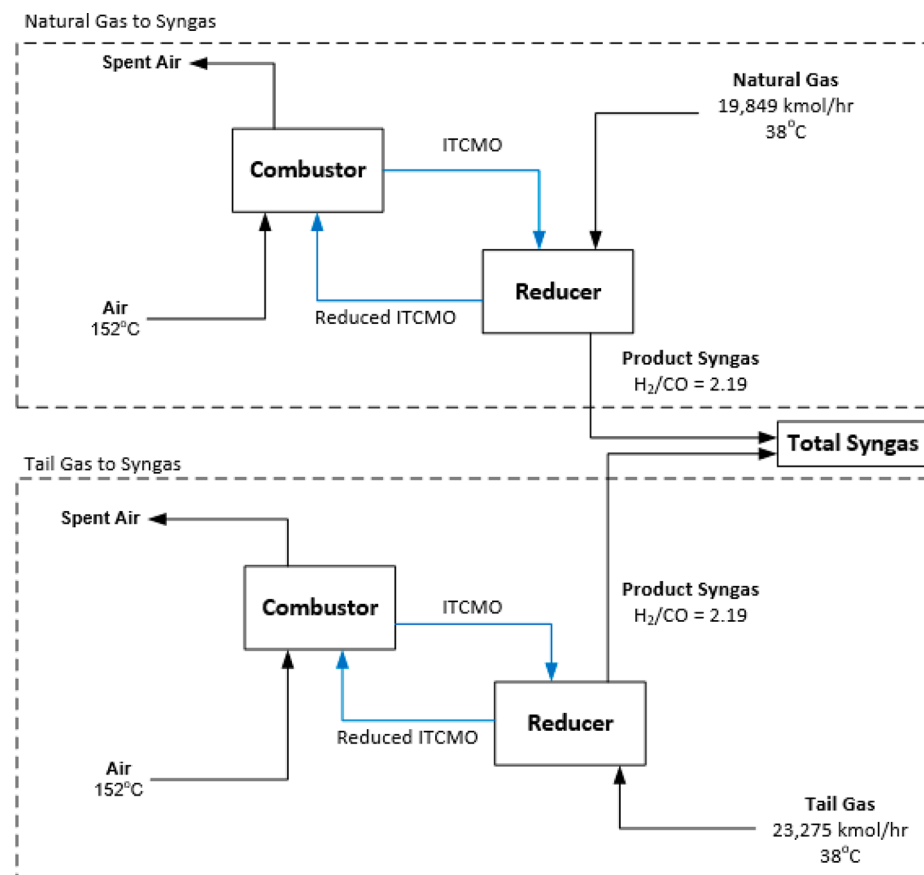


Figure 2. OSU MTS system with natural gas to syngas and tail gas to syngas in independent modules.

syngas to approach thermodynamic equilibrium. In practice, produced syngas needs to be conditioned to a pressure near the operating pressure used in the downstream reactors. For example, Fischer–Tropsch for liquid fuels operates at a pressure between 10 and 35 atm and methanol synthesis operates between 40 and 100 atm.^{3,7,15–23} Production of syngas suitable for Fischer–Tropsch-based liquid fuel synthesis is considered in this process analysis.

Prior chemical looping processes at elevated pressure include the HYGAS process and carbon dioxide acceptor process. During the 1970s, the HYGAS process was developed by the Institute of Gas Technology (IGT).^{24,25} In the HYGAS process, coal char was gasified with air and steam at 76 atm to produce a reducing gas. The reducing gas then reacted with a partially oxidized iron-oxide-based metal oxide complex to reduce the iron oxide. The iron oxide was regenerated with steam in an oxidizer to produce H₂ at 76 atm. The HYGAS process was demonstrated in a large-scale, continuous operation, with a processing capacity of 75 tons per day of coal. The HYGAS process was never widely used commercially because its performance could not compete with the emerging natural gas to hydrogen processes as a result of incomplete fuel conversions and low metal oxide and particle reactivity.

Another high-pressure process also developed in the 1970s was the CO₂ acceptor process, which used a calcium-based sorbent to remove CO₂ from the syngas stream in a gasifier.²⁶ In the CO₂ acceptor process, coal was gasified with steam following the steam–carbon reaction. Simultaneously, a water-gas shift reaction produced H₂ and CO₂. CO₂ was removed by reaction with CaO to form CaCO₃. CaO was then regenerated

by calcining CaCO₃. This process was demonstrated at a pilot plant scale with an operating temperature and pressure between 800 and 1150 °C and 10 atm, respectively. Maintaining reactivity of the CaO sorbent over multiple cycles and a minimal sorbent purge per cycle are essential to the process economics, and attempts to improve the calcium chemical looping process are still ongoing.

More recently, OSU demonstrated a pilot-scale, pressurized syngas chemical looping (SCL) unit for hydrogen production from syngas at the National Carbon Capture Center (NCCC).^{14,27,28} The NCCC pilot-scale design uses three reactors, two counter-current moving beds and one fluidized bed, to produce hydrogen from syngas. The SCL pilot unit was operated at the 250 kW_{th} scale and 10 atm.

The redox kinetics for chemical looping reactions have been studied at elevated pressures. Fan et al. investigated the effect of the pressure on metal oxide kinetics in a thermogravimetric analyzer with a constant space velocity at varying pressures.^{29,30} It was found that increasing pressure has a positive effect on both reduction and oxidation kinetics of metal oxides when investigated under the same gas hourly space velocity. This study rectified the conclusion of the pressure effect on the redox kinetics from an earlier study by García-Labiano et al., in which they indicated instead a negative pressure effect in kinetics.³¹ This discrepancy was due to the earlier study failing to account for the change in gas dispersion and space velocity of the gas flow that occurs at higher pressures. The positive kinetic effects at higher pressures can lead to smaller reactor sizes.^{29,30,32,33} Fennell et al. recently studied the pressurized chemical looping kinetics, including kinetic modeling of iron

oxide and steam on the carbonation reaction with CaO.³³ They developed a predictive model of reaction kinetics up to a pressure of 5 atm for iron oxide and determined the kinetic-based expressions to gain insights into steam–calcium reactions.

Despite the need for providing syngas at elevated pressures, little is reported on thermodynamic syngas yields of a chemical looping system under elevated pressures. Previous studies have shown the adequacy of modeling a moving bed reactor performance at atmospheric conditions using equilibrium simulations.^{9,29} Further, the quantification of equilibrium conditions is a necessary first step in the design of any higher pressure system. This study focuses on evaluating the change in the syngas yield as a function of different pressures for a chemical looping system. Specifically, the behavior for syngas generation at elevated pressures is first quantified using an isothermal analysis. The results from the isothermal analysis are then used to set constraints for the adiabatic analysis, used for developing an autothermal chemical looping system. Simulation results and sensitivity studies are used to quantify the gaseous and solid compositions at the reactor outlet under various temperature and pressure conditions and gas inlet composition and to elucidate the effect of steam and CO₂ introduced as additional feedstock on product properties. The study shows operating conditions that allow thermodynamic syngas yields for elevated pressures to be comparable to those at atmospheric pressures.

2. PROCESS SIMULATION BASIS

The MTS reactor system is shown in Figure 2. The system has two reducers for producing syngas, one for natural gas and the other for tail gas. While a combined feed into a single reducer reactor would be considered in practice, the tail gas and natural gas feed are evaluated independently to characterize trends into syngas production from natural gas and tail gas. The composition and flow rate for natural gas and tail gas are given in Table 1 and obtained from a U.S. Department

Table 1. Natural Gas and Tail Gas Composition³⁴

component	natural gas		tail gas	
	molar flow (kmol/h)	molar fraction	molar flow (kmol/h)	molar fraction
CH ₄	18479.42	0.9310	742.54	0.0319
H ₂ O			30.26	0.0013
CO			3212.27	0.1380
CO ₂	198.49	0.0100	230.44	0.0099
H ₂			9429.64	0.4051
N ₂	317.58	0.0160	9327.22	0.4007
C ₂ H ₆	635.17	0.0320	102.42	0.0044
C ₃ H ₈	138.94	0.0070	107.08	0.0046
C ₂ H ₄			6.98	0.0003
C ₃ H ₆			13.97	0.0006
n-C ₄ H ₈			46.55	0.0020
n-C ₄ H ₁₀	79.40	0.0040	16.29	0.0007
i-C ₄ H ₁₀			9.31	0.0004
total	19849.00	1.0000	23275.00	1.0000

of Energy (DOE) report.³⁴ The system pressure was investigated between 1 and 30 atm. The inlet temperatures for natural gas, tail gas, steam, CO₂, H₂O, and air are highly conservative values that are set equal to the reference inlet temperatures from the DOE report to maintain consistency: 38 °C for natural gas, tail gas, and CO₂, 343 °C for steam, and 152 °C for air.³⁴ The metal oxide oxygen carrier is an iron–titanium composite metal oxide (ITCMO), which has been

shown to sustain reactivity and strength in long-term testing.³⁵ The ratio of Fe₂O₃/TiO₂ in ITCMO can vary and determines the Fe₂O₃/C ratio and the TiO₂ weight support percentage, wherein excess TiO₂ serves as an inert heat carrier to maintain reactor temperatures. The ITCMO chemistry has been validated using experimental results at atmospheric pressure conditions and a gas–solid reactor that achieves equilibrium conditions.^{8,9,30} Because the experimental results match the equilibrium composition, the simulations at a higher pressure are compared to those at 1 atm. The syngas is tuned to a H₂/CO ratio of 2.19 for the final comparison in this study, consistent with a cobalt-based Fischer–Tropsch synthesis.¹⁷⁰

3. ISOTHERMAL ANALYSIS

Aspen Plus process simulation software from AspenTech was used to model the MTS process. The specifics of the property methods and component lists can be found in the Supporting Information. Both the reducer and combustor reactor were modeled using the RGIBBS reactor module, which minimizes the Gibbs free energy of the specified components. Experimental results have confirmed that a RGIBBS reactor can accurately model the MTS process.^{30,36–38} The isothermal simulations follow a consistent methodology. The fuel input was fixed as given in Table 1. The temperature of the reducer and combustor were identical and varied from 850 to 1150 °C with an interval of 100 °C. The pressure of the reducer and combustor were also identical and analyzed at 1, 10, 24, and 30 atm. For a specific temperature and pressure, the ITCMO, H₂O, and CO₂ inputs were varied within the limits shown in Table 2. Important metrics are quantified, including the total syngas yield, methane conversion, and H₂/CO ratio. For simplicity, only a subset of the data is provided in detail.^{188 t2}

Table 2. Controlled Variables in Simulation Methodology

parameter varied	range	interval
temperature (°C)	850–1150	100
pressure (atm)	1–30	1, 10, 24, and 30
ITCMO (molar ratio: Fe ₂ O ₃ /C _{in})	0–3	5 × 10 ⁻³
H ₂ O (molar ratio: H ₂ O/C _{in})	0–4	1.25 × 10 ⁻³
CO ₂ (molar ratio: CO ₂ /C _{in})	0–4	1.25 × 10 ⁻³

3.1. Natural Gas Isothermal Investigation. **3.1.1. Effect of Fe₂O₃ Flow.** The effect of Fe₂O₃ (ITCMO) on syngas production without the addition of steam or CO₂ was initially investigated. Considering only the gaseous species of the stoichiometric reaction, wherein 1 mol of CH₄ becomes 2 mol of H₂ and 1 mol of CO, it is expected that an increasing pressure decreases the amount of syngas produced as a result of volume expansion of the reaction. The trends for syngas generation using ITCMO only are compared for their syngas yields (Figure 3), methane conversion (Figure 4), and H₂/CO molar ratio (Figure 5).^{199 fs f4}

Figure 3 shows the effect of the pressure and reducer temperature on the specific syngas yield (H₂ + CO/carbon_{in}), and there is a clear decrease with an increasing pressure. At higher temperatures, there is less of a decrease in syngas production compared to lower temperatures when increasing the pressure. For example, in the range of constant syngas production (corresponding to Fe/FeO equilibrium), in comparison between a pressure of 1 and 30 atm, there is a 1.5% decrease in the syngas yield at 1150 °C and a 46% decrease in the syngas yield at 850 °C.²⁰⁹

The differences in syngas production performance between 1 and 30 atm can be understood by considering the syngas

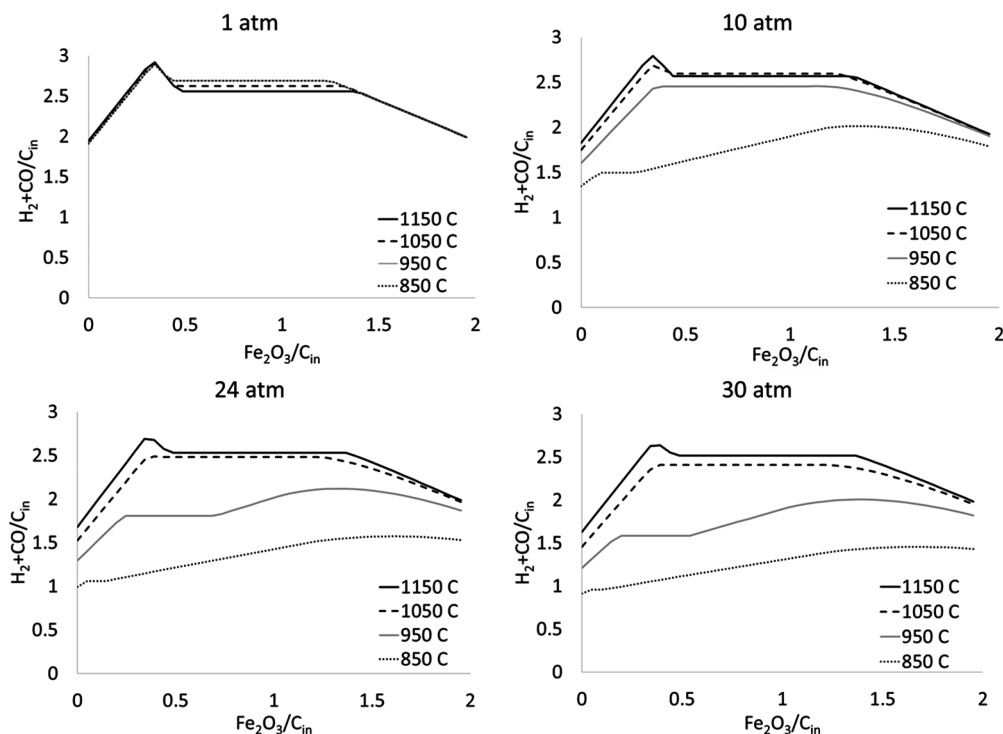


Figure 3. Specific syngas yield versus specific Fe_2O_3 flow at pressures of 1, 10, 24, and 30 atm for isothermal simulations from 850 to 1150 °C.

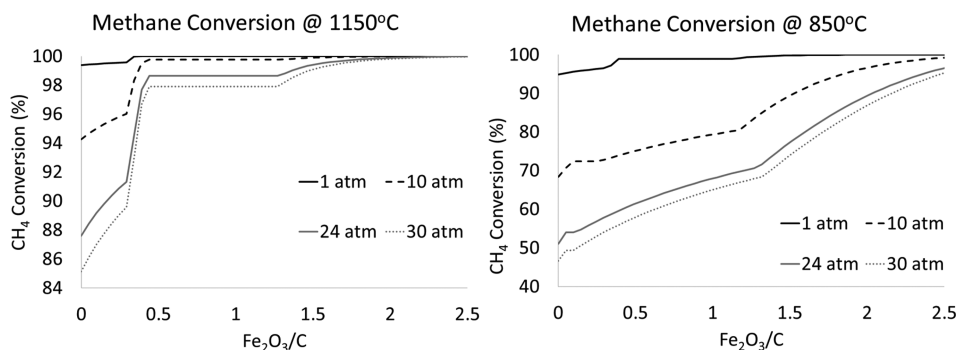


Figure 4. Methane conversion versus normalized Fe_2O_3 input at pressures of 1, 10, 24, and 30 atm at (left) 850 °C and (right) 1150 °C.

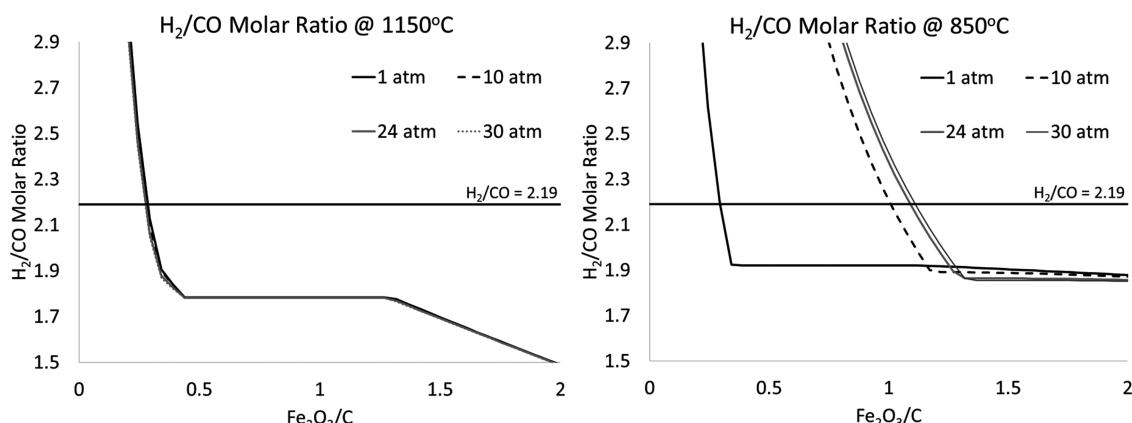


Figure 5. H_2/CO molar ratio versus Fe_2O_3/C input at pressures of 1, 10, 24, and 30 atm for isothermal simulations at (left) 850 °C and (right) 1150 °C.

generation trend at 850 °C and 1 atm. Initially, syngas production increases with increasing Fe_2O_3 flow, followed by a range where syngas production remains constant (correspond-

ing to Fe/FeO) at equilibrium composition with an increasing Fe_2O_3 flow. At 1 atm and 850 °C, the initial increase in the syngas yield (Figure 3) is with an increasing conversion of

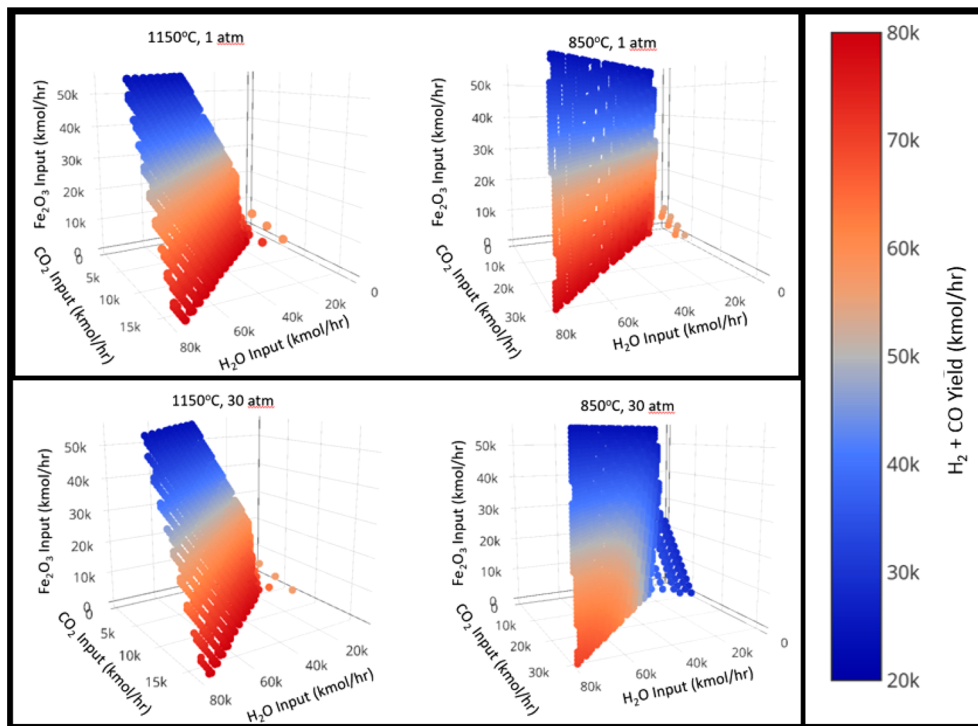


Figure 6. Syngas yield and H_2/CO equal to 2.19 versus H_2O input, CO_2 input, and Fe_2O_3 input at (top left) 1150 °C and 1 atm, (top right) 850 °C and 1 atm, (bottom left) 1150 °C and 30 atm, and (bottom right) 850 °C and 30 atm.

solid carbon as more lattice oxygen is introduced in the system via increasing Fe_2O_3 flow rates. After the initial increase, the syngas production stays constant for a certain range of Fe_2O_3 flow rates. In this operating range, the excess lattice oxygen in the reducer reactor converts Fe to FeO , enabling the syngas composition to stay constant. As the Fe_2O_3 flow rate is increased further, the transition from Fe to FeO is complete and excess oxygen in the system is used to convert H_2 to H_2O and CO to CO_2 , decreasing the syngas yields.

In comparison of syngas production at 850 °C between 1 and 30 atm, it is seen that syngas production as a function of increasing specific Fe_2O_3 flow ($Fe_2O_3/\text{carbon}_{in}$) follows the same general trend, although at a lower syngas yield magnitude. The lower syngas magnitude at 30 atm ($T = 850$ °C) can be explained by considering Figures 3 and 4 in conjunction. At 850 °C and 1 atm, the maximum syngas yield occurs at a specific iron flow of 0.35, which corresponds to a methane conversion of 97%. For the same condition at 30 atm, the methane conversion reduces to 55% but the specific iron flow no longer corresponds to the maximum syngas yield, which occurs at 1.6. This is driven by the fact that methane conversion continually increases from 55 to 98% with an increasing specific Fe_2O_3 flow rate at 30 atm, in contrast to near complete methane conversion at all Fe_2O_3 flow rates for 1 atm. The increase in the specific flow rate of Fe_2O_3 increases methane conversion and syngas yield, but beyond a certain point, the syngas yields drop as H_2 and CO begin to be converted to H_2O and CO_2 . This results in a single specific Fe_2O_3 flow rate (of 1.6), which gives the maximal syngas yield. This comparison of syngas generation trends illustrates the delicate balance between the temperature, Fe_2O_3 flow, syngas yield, and methane conversion when operating at elevated pressures that must be considered when selecting the reducer operating conditions.

In general, for a given pressure, there is a threshold temperature above which the trend is sharp and well-defined and syngas production yields are similar for 1 and 30 atm. Below the threshold temperature, as pressure increases, there exists a maxima in syngas production that is obtained by a balance of increasing methane conversion and increasing specific Fe_2O_3 flow rate.

The H_2/CO ratio is the final consideration for selecting an operating condition. Figure 5 shows the variation of the H_2/CO molar ratio in syngas. Considering methane conversion and syngas yield, at 850 °C, the selection of an operating point becomes fairly easy at 1 atm, because there are a wide range of variables with high syngas production and high methane conversion. Selection of an operating point becomes much more difficult at 30 atm, as the peak syngas is achieved at 77% methane conversion. At 850 °C, the restriction of H_2/CO ratio to 2.19 yields an Fe_2O_3/C operating condition that is lower than the maximum syngas yield from Figure 3, and hence, H_2O and CO_2 co-injection with Fe_2O_3 input is considered.

3.1.2. Effect of Fe_2O_3 Input and H_2O and CO_2 Co-injection. The ultimate goal of the isothermal investigation is to find operating conditions such that the syngas produced from natural gas meets the downstream requirements, namely, a H_2/CO ratio equal to 2.19. By simultaneous variation of the H_2O , CO_2 , and Fe_2O_3 inputs for design values shown in Table 2, the isothermal analysis is expanded to acquire a set of points that yield a product gas H_2/CO ratio equal to 2.19. Defining any two of the variables under the requirement of a H_2/CO ratio of 2.19 offers only one possible value for the third variable. Similarly, defining the system in the same manner as above, each of these defined points corresponds to a syngas yield ($H_2 + CO$). Therefore, the change in the syngas yield for varying H_2O , CO_2 , and Fe_2O_3 can be plotted wherein the H_2/CO ratio is 2.19, as shown in Figure 6, revealing several

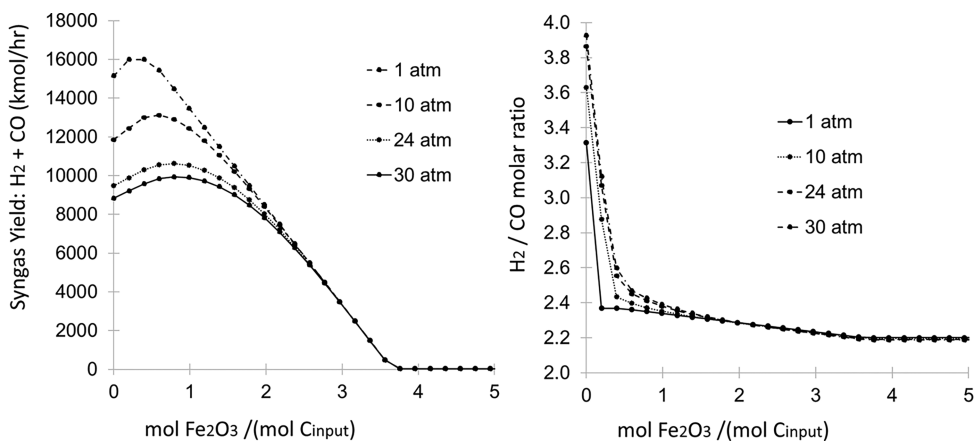


Figure 7. (Left) Syngas yield and (right) H₂/CO molar ratio versus normalized Fe₂O₃ input at 850 °C for isothermal simulations at pressures of 1, 10, 24, and 30 atm.

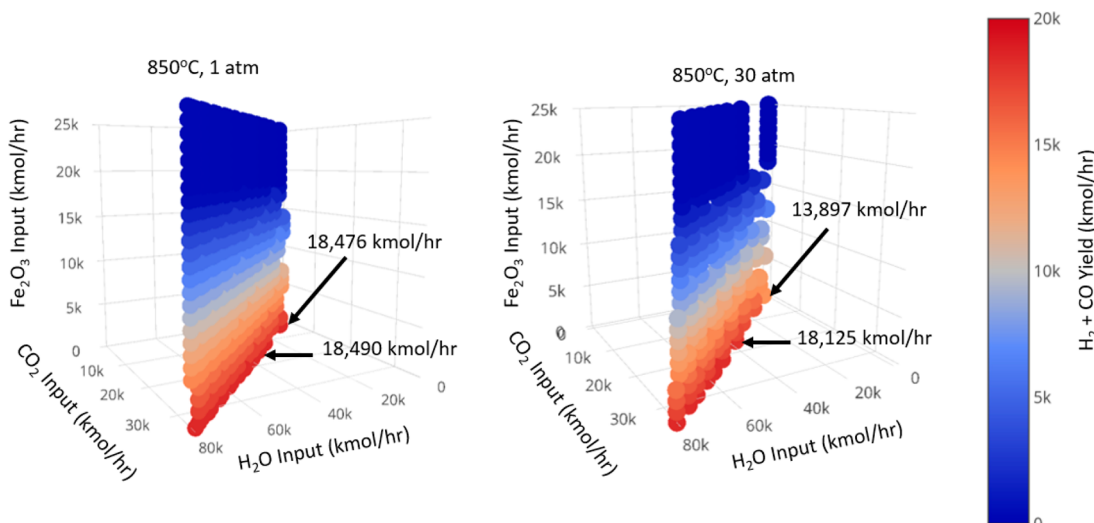


Figure 8. Syngas yield with H₂/CO equal to 2.19 versus H₂O input, CO₂ input, and Fe₂O₃ input at (left) 850 °C and 1 atm and (right) 850 °C and 30 atm.

noteworthy trends. First, the H₂O input will always be greater than the CO₂ input because the innate H₂/C ratio of methane is 2.0; therefore, an additional hydrogen source, steam in this case, is necessary to increase the ratio to 2.19. Second, a decrease in Fe₂O₃ leads to an increase in the syngas yield. Thermodynamically, methane will react with oxygen in Fe₂O₃ to form a reduced form of the metal oxide. In the absence of sufficient Fe₂O₃, methane will use H₂O or CO₂ as the oxygen source, resulting in additional H₂ or CO generation. While this method is beneficial in an isothermal system, the reduction of H₂O and CO₂ are highly endothermic, requiring a heat source to maintain the reactor temperature. The reaction of Fe₂O₃ with methane offers the capacity to offset the endothermic heat for CO₂ and H₂O reduction reactions by the regeneration reaction in the combustor reactor, resulting in a potential autothermal operation of the system. Lastly, the presence of H₂O and CO₂ decrease the effect that higher pressures have on the syngas yield. Comparing the results at 850 °C and 1 and 30 atm show that both reach a near peak value with high H₂O and CO₂ inputs; however, there is a notable decrease in the syngas yield at low H₂O and CO₂ input flows at 30 atm. This demonstrates that a lack of sufficient gaseous co-injection results in decreasing syngas yields for a constant Fe₂O₃ value.

3.2. Tail Gas Isothermal Analysis. The tail gas composition is provided in Table 1, and several analogous trends to the natural gas investigation are given. Figure 7 shows the syngas generation trends using Fe₂O₃ without CO₂ and H₂O at 850 °C. The syngas yield increases to a maxima with the peak syngas yield occurring at an increasing specific Fe₂O₃ flow with increasing pressure. The trend in syngas yield follows a trend similar with respect to the pressure; however, the difference between operation at 1150 and 850 °C is significantly lesser than that of Figure 3. This is a result of the large volume percentage of either unreactive or product gases in the tail gas stream. Approximately 40% of tail gas is N₂, and another 54% is syngas, leaving a small volume of gas relative to the total gas volume available to form syngas and undergo the corresponding gas expansion. From Figure 7, there are no points of operation that correspond to a H₂/CO ratio of 2.19 and high syngas yields. This is because the tail gas already has a H₂/CO ratio of 2.935; therefore, the system requires CO₂ input to achieve a H₂/CO ratio of 2.19. In theory, the tail gas reactor could serve as a H₂-rich syngas, while the natural gas functions as a H₂-deficient syngas, such that the combined syngas H₂/CO ratio is 2.19. Such an analysis is outside the scope of this work.

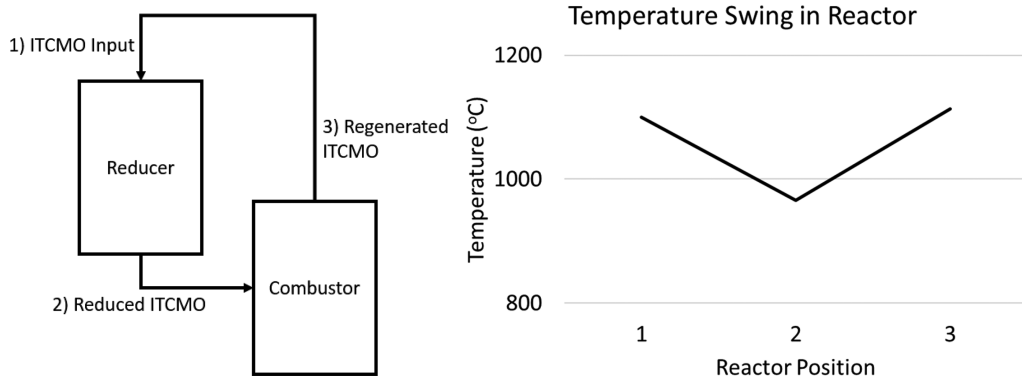


Figure 9. (Left) Positions of solids in the chemical looping reactor and (right) temperature at the corresponding reactor position for 35 000 kmol/h Fe_2O_3 with 85% TiO_2 weight support and 19 849 kmol/h natural gas input.

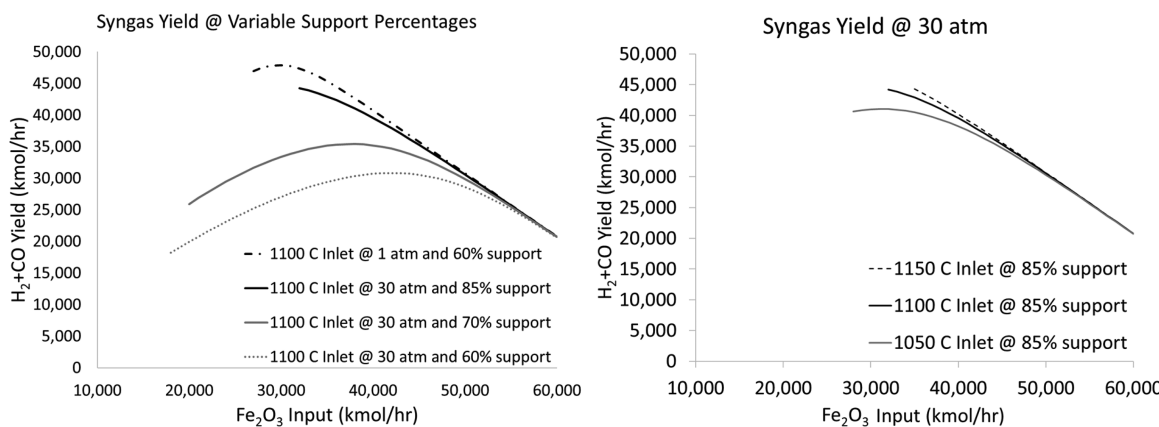


Figure 10. $\text{H}_2 + \text{CO}$ yields versus Fe_2O_3 input as a function of solids inlet temperature with 10 000 kmol/h steam input and no solid carbon formation for (left) varying TiO_2 weight supports and (right) varying solids inlet temperatures with 85% TiO_2 support.

332 **3.2.1. Syngas Generation Trends with Fe_2O_3 Input and**
 333 **H_2O and CO_2 Co-injection.** The H_2O and CO_2 input is varied
 334 within the specifications shown in Table 2. From the
 335 isothermal analysis for tail gas, the syngas yields for 1 and 30
 336 atm systems are similar at higher temperatures, while the
 337 differences in syngas yields are larger at lower temperatures.
 338 Hence, it is worthwhile to compare syngas yields at the lower
 339 temperature of 850 °C at 1 and 30 atm. Figure 8 shows the
 340 variation of syngas yields for a given Fe_2O_3 input as a function
 341 of steam and CO_2 injection at a constant H_2/CO ratio of 2.19.
 342 The syngas yield for steam and CO_2 injection follows a trend
 343 similar to the natural gas analysis, where increasing the Fe_2O_3
 344 flow decreases the syngas yield. The syngas yield is also
 345 dependent upon $\text{H}_2\text{O}/\text{CO}_2$ co-injection, where a sufficiently
 346 high H_2O and CO_2 input is necessary at 30 atm to maintain
 347 high syngas yields. Further, at higher $\text{Fe}_2\text{O}_3/\text{C}_{\text{in}}$ flow rates, the
 348 syngas yield is near zero because the excess lattice oxygen in
 349 the reducer is used to convert partial oxidation products of CO
 350 and H_2 to full oxidation products of CO_2 and H_2O .

additional fuel for combustion (such as steam methane reformers) or provide additional oxygen from an air separation unit to combust with the natural gas (such as autothermal reforming or partial oxidation systems) to provide the necessary heat.^{3–5} Chemical looping avoids both additional fuel combustion and the use of an air separation unit because the metal oxide oxygen carrier also serves as the heat transfer medium to transfer heat from the combustor to the reducer. The adiabatic chemical looping system is operated under the condition in which the inlet temperature of the oxygen carrier to the reducer is greater than the outlet temperature, with the temperature drop providing the heat for syngas generation. In the combustor reactor, the reduced metal oxide oxygen carrier is reoxidized with air with its temperature raised to regenerate the heat lost. For the adiabatic analyses, the excess air in the combustor was set at 5%. The reoxidation reaction is exothermic, and a portion of the heat goes to increasing the temperature of the metal oxide to a temperature greater than the reducer outlet. This temperature swing is shown in Figure 9, where ITCMO enters at 1100 °C (position 1), exists in the reducer (position 2) at ~950 °C, and exits the combustor at ~1110 °C (position 3). The temperature of the oxygen carrier at position 3 being greater than or equal to position 1 allows for the MTS process to operate autothermally. Those conditions that satisfy the temperature swing condition are a solution set for operation of the MTS process.

The maximum syngas yield is significantly influenced by the heat balance of the process, which is controlled by the amount of preheat associated with the input streams. In the DOE

4. ADIABATIC REACTOR MODELING ANALYSIS AND DISCUSSION FOR NATURAL GAS

From Figure 6, the maximum isothermal syngas yield is around 80 000 kmol/h, corresponding to ~4 mol of syngas/mol of carbon input. When considering the heat balance, attaining this maximum value is not feasible in practice because generating syngas from natural gas with steam, CO_2 , and ITCMO is all endothermic. Conventional syngas generation systems may use

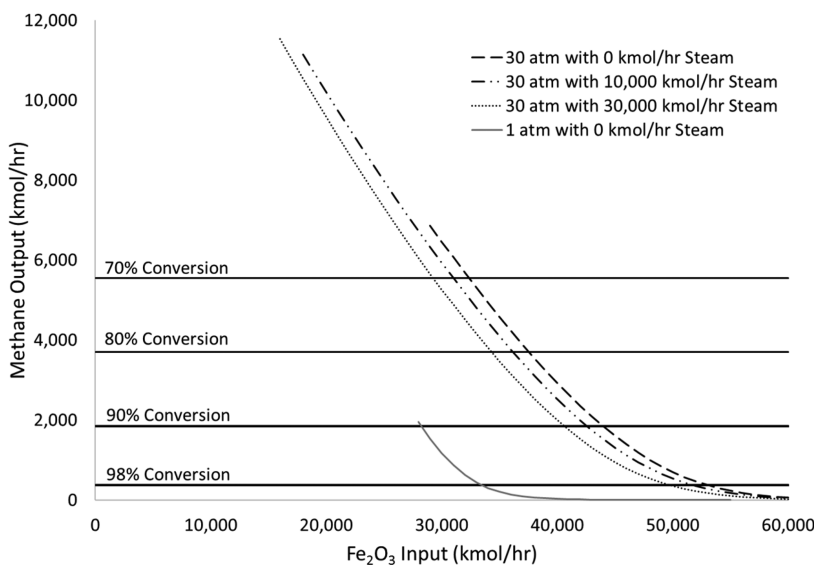


Figure 11. Methane output versus Fe_2O_3 input with varying steam input, no solid carbon formation, 60% TiO_2 weight support, and 1100 °C solids inlet at 1 and 30 atm.

387 report³⁴ from which natural gas flow rates and compositions
388 are chosen, the excess heat is used to generate electricity for
389 the air separation unit. Because the MTS process does not
390 require an air separation unit, there is potential for additional
391 internal heat integration between the spent air, combustor air,
392 and fuel and syngas streams. To maintain consistency, the
393 system preheat temperatures for the adiabatic system remain
394 identical to the isothermal system given in section 3. This leads
395 to the results being conservative but still useful in providing a
396 lower boundary for the performance of the MTS process.

397 **4.1. System Design Variables for Adiabatic Operation.** From the isothermal results, operating at a higher
398 temperature can compensate for the negative effect of the
399 pressure. A higher temperature can be obtained by increasing
400 the solids inlet temperature and TiO_2 weight support
401 percentage. In an adiabatic reducer, increasing the solids
402 inlet temperature and TiO_2 weight support percent both
403 increase the syngas yield but the Fe_2O_3 flow required to satisfy
404 the autothermal requirement also increases. This effect is
405 demonstrated in Figure 11, where the syngas yield as a
406 function of Fe_2O_3 flow is shown with a steam input of 10 000
407 kmol/h, no solid carbon formation, and a variable H_2/CO
408 ratio. On the basis of reaction kinetics and cyclic reactivity, the
409 lower and upper bounds for the solids inlet temperature are
410 850 and 1150 °C, respectively. For a given TiO_2 weight
411 support percentage, a higher solids inlet temperature results in
412 a higher peak syngas production. However, the autothermal
413 operating condition can be satisfied at a lower solids flux at
414 lower temperatures. This leads to a trade-off between syngas
415 production and ITCMO flow that must be balanced. This can
416 be seen in Figure 10, where only ITCMO flow rates that satisfy
417 the autothermal condition are shown.

418 The left panel of Figure 10 shows that, as the TiO_2 support
419 percentage is increased from 60 to 85%, the syngas yield values
420 at 30 atm follow a trend similar to that at 1 atm. At 30 atm and
421 85% TiO_2 support, the syngas yield values are similar to those at
422 1 atm. Further, syngas yields at 30 atm show an increase with
423 increasing reducer solids inlet temperatures, as shown in the
424 right panel of Figure 10. Increasing the ITCMO flow increases
425 the methane conversion. However, the maximum conversion

426 of methane and maximum syngas yield do not correspond to
427 the same inlet conditions. Therefore, when an operating
428 condition is selected, it is important to understand how the
429 methane conversion impacts the system performance. Figure
430 11 shows the methane output versus Fe_2O_3 input at a TiO_2
431 support of 60 wt % with varying steam injection, no solid
432 carbon formation, and autothermal operating conditions.
433 Figure 11 is shown at 60 wt % to enable better visualization
434 of trends because the results at 85 wt % are similar but with a
435 lower magnitude. From the data at 30 atm in Figures 10 and
436 11, there will be a greater amount of unconverted methane at
437 peak syngas production. The tolerance of unconverted
438 methane is dependent upon the downstream processing
439 steps. It may, for example, be necessary to operate the reactor
440 at a higher flow rate of ITCMO such that unconverted
441 methane is below a threshold value but at the expense of a
442 lower syngas yield. Methane conversion is highly dependent
443 upon the temperature and pressure, with the pressure
444 decreasing methane conversion. This highlights one of the
445 main differences between syngas generation at pressure
446 compared to ambient.

447 The addition of steam increases the methane conversion,
448 which is shown in the 30 atm data of Figure 11, with steam
449 values ranging from 0 to 30 000 kmol/h of steam. This is more
450 pronounced at higher pressures where using steam because an
451 additional oxidant can reduce the effect of volume expansion.
452 At higher ITCMO flow rates, the effect of steam on improving
453 methane conversion decreases as a result of the increase in
454 oxygen supplied by ITCMO. Steam also has an additional
455 benefit in that it reduces the ITCMO required to satisfy an
456 autothermal heat balance to a certain extent as it increases
457 methane conversion. However, the presence of steam does
458 decrease the syngas purity and adds an additional processing
459 step because the excess steam would require removal.
460 Analogous to steam, CO_2 injection shows a similar trend.

461 **4.2. Adiabatic Operation for Natural Gas Feedstock with Fe_2O_3 Input and H_2O and CO_2 Co-injection.** Isothermal conditions, a higher temperature, and the addition of H_2O and CO_2 improve the syngas yield and methane conversion. Section 4.1 concludes that a greater TiO_2 weight

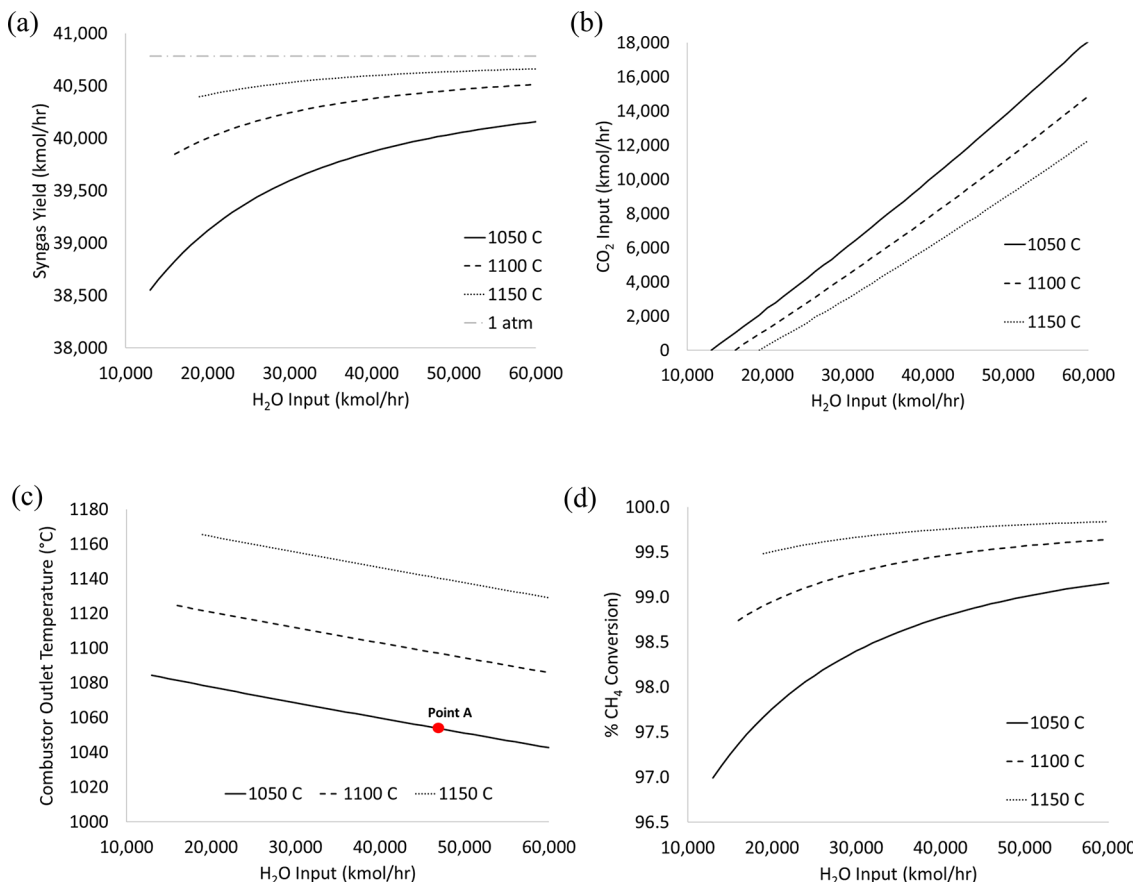


Figure 12. Fe_2O_3 flow rate of 40 000 kmol/h and operating pressure of 30 atm: (a) variation of the syngas yield with increasing H_2O input flow rates, (b) CO_2 input flow rates that correspond to a given H_2O input flow rate for obtaining a H_2/CO ratio of 2.19, (c) combustor outlet temperature as a function of an increasing H_2O input flow rate, and (d) methane conversion as a function of an increasing H_2O input flow rate.

percent support in ITCMO enables a higher syngas yield. To investigate the effect of H_2O and CO_2 under adiabatic conditions, the TiO_2 weight percent support was maintained at 85% and the MTS process was analyzed at three ITCMO inlet temperatures to the reducer (1150, 1100, and 1050 °C). For a given ITCMO flow rate, inlet ITCMO temperature, and reducer pressure, the CO_2 and H_2O flows were varied to obtain a H_2/CO ratio of 2.19. Additional constraints that must be satisfied for an operating condition to be considered viable include the inlet temperature of the solids into the reducer being greater than the combustor outlet temperature, a high methane conversion constraint (>95%), a syngas yield within 10% of that produced at 1 atm, and a low solid carbon formation. The approach for determining operating conditions that satisfy the H_2/CO molar ratio, methane conversion, and autothermal operation region at each ITCMO flow rate is demonstrated using Figure 12. All of the conditions shown in Figure 12 refer to syngas produced at 30 atm with a H_2/CO molar ratio of 2.19 and a fixed ITCMO flow rate corresponding to 40 000 kmol/h of Fe_2O_3 . For a given reducer inlet temperature, panels a–d of Figure 12 show the (a) impact of steam on the syngas yield, (b) CO_2 required to maintain H_2/CO of 2.19, (c) combustor outlet temperature, and (d) methane conversion. Figure 12 shows that, for all temperatures, the (a) syngas yield and (d) methane conversion increase with an increasing H_2O flow. For a given H_2O flow and with a fixed ITCMO flow, there is only one unique CO_2 flow rate that will yield a H_2/CO ratio of 2.19 (Figure 12b).

The upper limit on H_2O flow at a given solids inlet temperature is demonstrated using point A in Figure 12c. For a reducer inlet temperature of 1050 °C, point A corresponds to the H_2O flow rate when the combustor outlet temperature is 1050 °C. As the H_2O flow rate increases beyond point A, no operating conditions will satisfy an autothermal heat balance because the combustor outlet temperature of solids will be lower than the reducer inlet temperature of 1050 °C. There is an inverse relationship between the maximum H_2O flow rate and ITCMO inlet temperature. Increasing the ITCMO inlet temperature decreases the maximum flow of H_2O , where the autothermal heat balance criteria is satisfied.

The conditions that satisfy the autothermal operating conditions via the method in Figure 12 are characterized for different ITCMO flow rates and summarized in panels a–c of Figure 13. Panels a–c of Figure 13 show the variation of syngas yields, H_2O flow, and methane conversion at 30 atm for varying ITCMO flow rates. Figure 13a shows that the syngas yield increases with a decreasing ITCMO flow and an increasing temperature. Further, whenever there is a feasible autothermal operating condition, a higher reducer inlet temperature results in a higher syngas yield (Figure 13a), lower H_2O flow (Figure 13b), and higher methane conversion (Figure 13c). However, the lowest Fe_2O_3 input that can achieve an autothermal operation is limited for a higher reducer inlet temperature. For example, at a reducer inlet temperature of 1150 °C, the syngas yield is higher and the

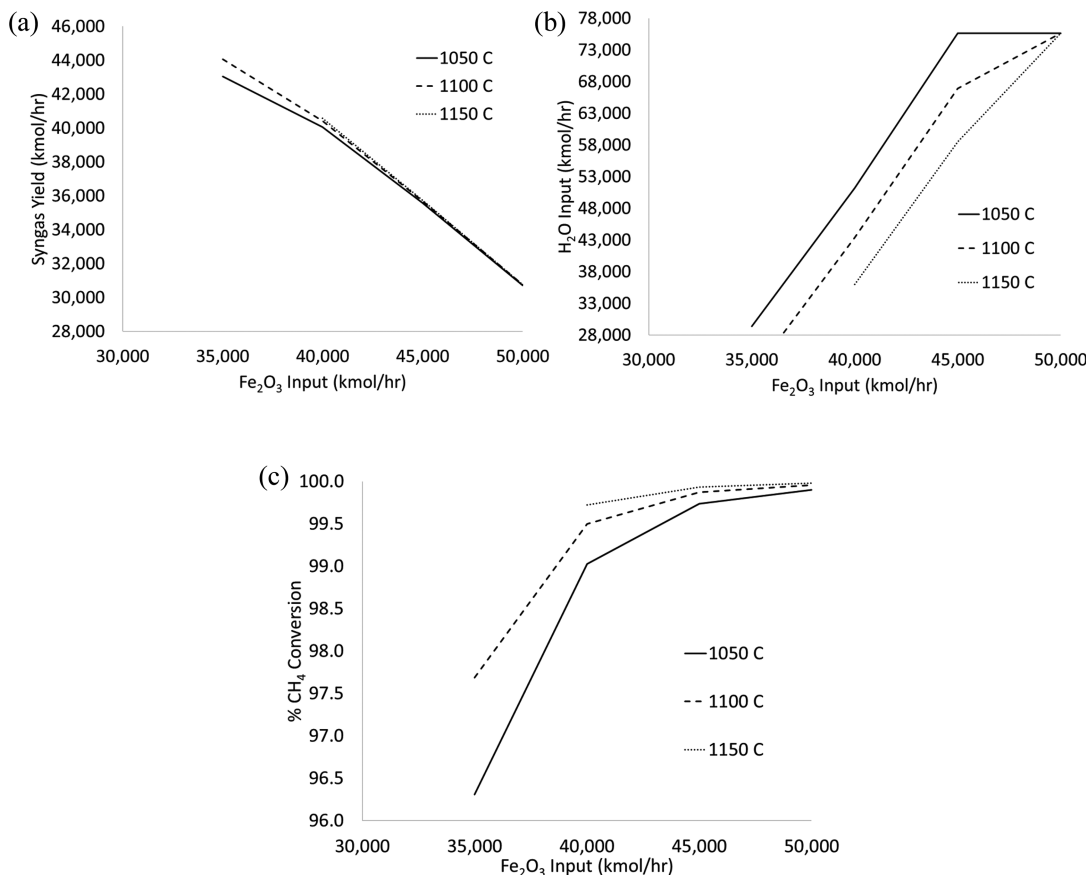


Figure 13. Operating pressure of 30 atm and natural gas feedstock: (a) variation of the maximum syngas yield with decreasing Fe_2O_3 input flow rates, (b) variation of H_2O input flow rates as a function of decreasing Fe_2O_3 input flow rates for a maximum syngas yield, and (c) methane conversion as a function of the Fe_2O_3 flow rate.

Table 3. Summary of Operating Conditions and Yields for Input of Steam, CO_2 , Fe_2O_3 (ITCMO), and Solids Temperatures for High Syngas Yield at 1 and 30 atm Using Natural Gas as the Feedstock

case	pressure (atm)	system input						CH_4 conversion (%)	$\text{H}_2 + \text{CO}$ (kmol/h)	specific syngas yield (mol/mol)
		solids inlet temperature (°C)	H_2O input (kmol/h)	CO_2 input (kmol/h)	Fe_2O_3 input (kmol/h)	specific Fe_2O_3 flow (mol/mol)				
A	1	1050	26600	6122	35000	1.71	100.0	45781	2.23	
B	1	1100	20200	2385	35000	1.71	100.0	45783	2.24	
C	30	1050	29400	7037	35000	1.71	96.3	43045	2.10	
D	30	1100	21600	2758	35000	1.71	97.7	44067	2.15	

s₂₃ steam consumption is lower than at reducer inlet temperatures s₂₄ of 1100 and 1050 °C, but no autothermal operating conditions s₂₅ exist for an Fe_2O_3 flow below 40 000 kmol/h. As the solids s₂₆ inlet temperature is reduced, the Fe_2O_3 flow necessary to s₂₇ achieve an autothermal heat balance is also reduced, creating a s₂₈ trade-off between the syngas yield, H_2O consumption, and s₂₉ ITCMO requirements. From the isothermal results in Figure 4, s₃₀ the methane conversion suffered a steep drop as a function of s₃₁ the pressure but was a strong function of specific Fe_2O_3 , steam, s₃₂ and CO_2 flows. From Figure 13c, methane conversion is always s₃₃ maintained above 95% when constraints are placed on the H_2/CO ratio and heat balance.

The operating conditions in Table 3 are summarized as a series of design cases that maximize the syngas yield from natural gas under autothermal conditions with an Fe_2O_3 flow rate of 35 000 kmol/h. Cases A and B represent design cases at 1 atm for solids inlet temperatures of 1050 and 1100 °C,

respectively. Cases C and D represent design cases at 30 atm for solids inlet temperatures of 1050 and 1100 °C, respectively. Full stream breakdowns of each design case are given in the Supporting Information.

It can be seen that, with the appropriate H_2O and CO_2 input, a syngas with a H_2/CO ratio of 2.19 and autothermal operation can be achieved with a syngas yield at 30 atm that is only modestly lower than the 1 atm case. For example, in comparison of the specific syngas yield in cases A and C (1050 °C solids inlet at 1 and 30 atm), the 30 atm operating condition results in a syngas yield within 6% of the 1 atm operating condition. Similarly, in comparison between cases B and D (1100 °C solids inlet at 1 and 30 atm), the 30 atm operating condition offers syngas yields within 5% of the 1 atm operating condition. With further refinements to the process conditions that consider the entire downstream process, such as increased preheat temperatures and using a combined

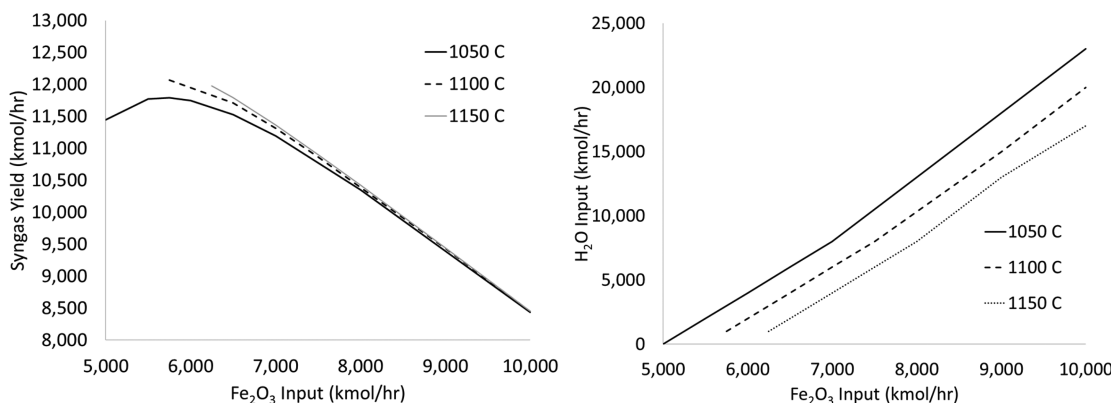


Figure 14. Operating pressure of 30 atm and tail gas feedstock: (left) variation of the maximum syngas yield with decreasing Fe₂O₃ input flow rates and (right) variation of H₂O input flow rates as a function of decreasing Fe₂O₃ input flow rates for the maximum syngas yield.

Table 4. Summary of Operating Conditions and Yields for Input of Steam, CO₂, Fe₂O₃ (ITCMO), and Solids Temperatures for High Syngas Yield at 1 and 30 atm Using Tail Gas as the Feedstock

case	pressure (atm)	system input				
		solids inlet temperature (°C)	H ₂ O input (kmol/h)	CO ₂ input (kmol/h)	Fe ₂ O ₃ input (kmol/h)	H ₂ + CO (kmol/h)
A1	1	1050	1986	809	5,750	12,706
B1	1	1100	264	17	5,750	12,707
C1	30	1050	3154	1219	5,750	11,801
D1	30	1100	1054	249	5,750	12,075

mixture of natural gas and tail gas as the fuel input, it is possible to generate syngas at elevated pressures that are comparable to ambient pressure while maintaining important conditions, such as a target H₂/CO ratio, autothermal heat balance, and practical solids flux.

4.3. Adiabatic Operation for Tail Gas Feedstock with Fe₂O₃ Input and H₂O and CO₂ Co-injection. For the tail gas system, a consistent methodology as that shown in Figure 12 is used to identify the maximum syngas yield at 30 atm. Figure 14 shows the syngas yield and steam requirements for the tail gas system under autothermal operating conditions. The syngas yield decreases with increasing ITCMO flow. Analogous to the analysis for Figure 13, at a given ITCMO flow rate, a higher reducer inlet temperature generates a higher syngas yield. Below an ITCMO flow rate of 6500 kmol/h, no conditions satisfy autothermal operating conditions at an ITCMO inlet temperature of 1150 °C. At an ITCMO flow of 5750 kmol/h, autothermal operation can be achieved at 1100 and 1050 °C. These high syngas yield values are summarized in Table 4. The syngas yield provides no solution below 5500 kmol/h when the ITCMO inlet temperature to the reducer is 1100 °C, while the syngas yield at an ITCMO inlet temperature of 1050 °C is lower than that at 6000 kmol/h, indicating that the solution at 6000 kmol/h is near the maximal syngas yield for the given preheats.

Table 4 summarizes the comparison between operating at 1 and 30 atm. In a series of design cases, analogous to those conducted in the previous section, the difference between syngas yields at 1 atm (cases A1 and B1) are within 7.5% of those conducted at 30 atm (cases C1 and D1). This again confirms that, with further refinements to the process conditions, it is possible to generate syngas at elevated pressures that are comparable to ambient pressure under the aforementioned system constraints. The full stream breakdown of cases A1–D1 are given in the Supporting Information. Additional case studies were performed on a co-injection of

natural gas and tail gas following a method similar to the individual cases, using a Fe₂O₃ flow of 40 000 kmol/h. The results of the case studies showed results similar to the individual study, wherein the 30 atm case was within 7.5 and 5% of the 1 atm case with solids inlet of 1050 and 1100 °C, respectively. This result is shown in the Supporting Information.

5. CONCLUDING REMARKS

This study investigated the thermodynamic design conditions for high-pressure chemical looping reforming systems using iron-based oxygen carriers for syngas generation. For a natural gas to syngas and a tail gas to syngas system at the high pressure of 30 atm, there exists a set of operating variables including solids flow rates, CO₂ input flow rates, H₂O input flow rates, TiO₂ support percentage, and solids inlet temperatures that can be adjusted to obtain syngas yields comparable to those obtained from atmospheric operation. Specifically, the sensitivity analyses conducted on the chemical looping system quantify several trade-off effects in reforming performance in terms of methane conversion and syngas yields. The isothermal analysis indicates that increased temperatures and H₂O/CO₂ injection can mitigate the adverse effects of higher pressure operation on syngas yields. This conclusion was used to guide the design space of the adiabatic study. Exploring this design space in the adiabatic analysis indicates that operating at too high of a solids inlet temperature renders the autothermal performance difficult to achieve without higher solids circulation rates. Additionally, with pressurized operation, the conversion of methane may peak at different conditions than those for high syngas generation yields. This result is demonstrated in the natural gas case study, in which, for a 95% methane conversion tolerance, the syngas yield at 30 atm was within 6% of the atmospheric operating condition. The comparable syngas yields offer direction for designing a chemical looping system at elevated pressures.

ASSOCIATED CONTENT**Supporting Information**

The Supporting Information is available free of charge on the ACS Publications website at DOI: [10.1021/acs.energyfuels.8b01834](https://doi.org/10.1021/acs.energyfuels.8b01834).

Common reactions that can be used to approximate the thermodynamic equilibrium, ASPEN simulation properties and databanks, detailed mass and energy balance tables for various adiabatic chemical looping cases under autothermal conditions, and summary of operating conditions and results for a combined natural gas and tail gas feedstock ([PDF](#))

AUTHOR INFORMATION**Corresponding Author**

*E-mail: fan.1@osu.edu.

ORCID 

Liang-Shih Fan: [0000-0002-2075-6505](https://orcid.org/0000-0002-2075-6505)

Author Contributions

[†]Peter Sandvik and Mandar Kathe contributed equally to this work and are co-first authors.

Notes

The authors declare no competing financial interest.

REFERENCES

- (1) U.S. Energy Information Administration (EIA), U.S. Department of Energy (DOE). *Short Term Energy Outlook*; EIA, DOE: Washington, D.C., May 2018.
- (2) U.S. Energy Information Administration (EIA), U.S. Department of Energy (DOE). *Levelized Cost and Levelized Avoided Cost of New Generation Resources in the Annual Energy Outlook 2018*; EIA, DOE: Washington, D.C., March 2018.
- (3) Noelker, K.; Johanning, J. Autothermal reforming: A flexible syngas route with future potential. *Proceedings of the Nitrogen and Syngas International Conference*; Bahrain, Feb 28–March 3, 2010.
- (4) Lyubovsky, M.; Roychoudhury, S.; LaPierre, R. Catalytic partial oxidation of methane to syngas at elevated pressures. *Catal. Lett.* **2005**, *99* (3–4), 113–117.
- (5) Rostrup-Nielsen, J. R. Production of synthesis gas. *Catal. Today* **1993**, *18* (4), 305–324.
- (6) National Energy Technology Laboratory (NETL), U.S. Department of Energy (DOE). *Syngas Optimized for Intended Products*; NETL, DOE: Pittsburgh, PA, 2016.
- (7) Wilhelm, D. J.; Simbeck, D. R.; Karp, A. D.; Dickenson, R. L. Syngas production for gas-to-liquids applications: Technologies, issues and outlook. *Fuel Process. Technol.* **2001**, *71* (1–3), 139–148.
- (8) Kathe, M.; Empfield, A.; Sandvik, P.; Fryer, C.; Zhang, Y.; Blair, E.; Fan, L.-S. Utilization of CO₂ as a partial substitute for methane feedstock in chemical looping methane-steam redox processes for syngas production. *Energy Environ. Sci.* **2017**, *10* (6), 1345–1349.
- (9) Kathe, M.; Fryer, C.; Sandvik, P.; Kong, F.; Zhang, Y.; Empfield, A.; Fan, L.-S. Modularization strategy for syngas generation in chemical looping methane reforming systems with CO₂ as feedstock. *AIChE J.* **2017**, *63* (8), 3343–3360.
- (10) Fan, L.-S. *Chemical Looping Partial Oxidation: Gasification, Reforming, and Chemical Syntheses*; Cambridge University Press: Cambridge, U.K., 2017.
- (11) Adanez, J.; Abad, A.; Garcia-Labiano, F.; Gayan, P.; de Diego, L. F. Progress in chemical-looping combustion and reforming technologies. *Prog. Energy Combust. Sci.* **2012**, *38* (2), 215–282.
- (12) Fennell, P. Calcium and chemical looping technology: An introduction. *Calcium and Chemical Looping Technology for Power Generation and Carbon Dioxide (CO₂) Capture*; Woodhead Publishing: Sawston, U.K., 2015; pp 3–14.
- (13) Fan, L.-S.; Li, F. Chemical looping technology and its fossil energy conversion applications. *Ind. Eng. Chem. Res.* **2010**, *49* (21), 690 10200–10211.
- (14) Fan, L.-S. *Chemical Looping Systems for Fossil Energy Conversions*; John Wiley & Sons: Hoboken, NJ, 2011.
- (15) Wood, D.; Nwaoha, C.; Towler, B. Gas-to-liquids (GTL): A review of an industry offering several routes for monetizing natural gas. *J. Nat. Gas Sci. Eng.* **2012**, *9*, 196–208.
- (16) de Clerk, A. Gas-to-liquids conversion. *Proceedings of the Natural Gas Conversion Technologies Workshop of ARPA-E*; Houston TX, Jan 13, 2012.
- (17) Malik, A.; Mantri, V. *Gas-to-Liquids Plants Face Challenges in the U.S. Market*; U.S. Energy Information Administration (EIA), U.S. Department of Energy (DOE): Washington, D.C., 2014.
- (18) Goellner, J. F.; Kuehn, N. J.; Shah, V.; White, C. W., III; Woods, M. C. *Baseline Analysis of Crude Methanol Production from Coal and Natural Gas*; National Energy Technology Laboratory (NETL), U.S. Department of Energy (DOE): Pittsburgh, PA, 2014; DOE/NETL-341/101514.
- (19) Chmielniak, T.; Sciazko, M. Co-gasification of biomass and coal for methanol synthesis. *Appl. Energy* **2003**, *74* (3–4), 393–403.
- (20) Yoon, H.; Erickson, P. Hydrogen from coal-derived methanol via autothermal reforming processes. *Int. J. Hydrogen Energy* **2008**, *33* (1), 57–63.
- (21) Kathe, M.; Sandvik, P.; Fryer, C.; Kong, F.; Zhang, Y.; Grigoris, G.; Fan, L.-S. Coal refining chemical looping systems with CO₂ as a co-feedstock for chemical syntheses. *Energy Fuels* **2018**, *32* (2), 1139–1154.
- (22) Cheng, W. H. *Methanol Production and Use*; CRC Press: Boca Raton, FL, 1994.
- (23) Lin, H.; Jin, H.; Gao, L.; Han, W. Economic analysis of coal-based polygeneration system for methanol and power production. *Energy* **2010**, *35* (2), 858–863.
- (24) Biljetina, R.; Tarman, P. Development status of the steam–iron process for hydrogen production. *Altern. Energy Sources, [Proc. Miami Int. Conf.]*, **2nd** 1981, *8*, 3335–3347.
- (25) Institute of Gas Technology (IGT). *Development of the Steam–Iron Process for Hydrogen Production*; U.S. Department of Energy (DOE): Washington, D.C., 1979; EF-77-C-01-2435.
- (26) Dobbyn, R. C.; Ondik, H. M.; Willard, W. A.; Brower, W. S.; Feinberg, I. J.; Hahn, T. A.; Hicho, G. E.; Read, M. E.; Robbins, C. R.; Smith, J. H. *Evaluation of the Performance of Materials and Components Used in the CO₂ Acceptor Process Gasification Pilot Plant*; U.S. Department of Energy (DOE): Washington, D.C., 1978; AC01-76ET10253.
- (27) Fan, L.-S.; Zeng, L.; Wang, W.; Luo, S. Chemical looping processes for CO₂ capture and carbonaceous fuel conversion—prospect and opportunity. *Energy Environ. Sci.* **2012**, *5* (6), 7254–7280.
- (28) Hsieh, T.-L.; Xu, D.; Zhang, Y.; Nadgouda, S.; Wang, D.; Chung, C.; Pottimurthy, Y.; Guo, M.; Chen, Y.-Y.; Xu, M.; He, P.; Fan, L.-S.; Tong, A. 250 kW_{th} high pressure pilot demonstration of the syngas chemical looping system for high purity H₂ production with CO₂ capture. *Appl. Energy* **2018**, *230*, 1660–1672.
- (29) Deshpande, N.; Majumder, A.; Qin, L.; Fan, L.-S. High-pressure redox behavior of iron-oxide-based oxygen carriers for syngas generation from methane. *Energy Fuels* **2015**, *29* (3), 1469–1478.
- (30) Luo, S.; Zeng, L.; Xu, D.; Kathe, M.; Chung, E.; Deshpande, N.; Qin, L.; Majumder, A.; Hsieh, T.-L.; Tong, A.; Sun, Z.; Fan, L.-S. Shale gas-to-syngas chemical looping process for stable shale gas conversion to high purity syngas with a H₂:CO ratio of 2:1. *Energy Environ. Sci.* **2014**, *7* (12), 4104–4117.
- (31) García-Labiano, F.; Adanez, J.; de Diego, L. F.; Gayan, P.; Abad, A. Effect of pressure on the behavior of copper-, iron-, and nickel-based oxygen carriers for chemical-looping combustion. *Energy Fuels* **2006**, *20* (1), 26–33.
- (32) Deshpande, N. Calcium and Iron Oxide Reactivity Studies for Chemical Looping Applications of Clean Energy Conversion.

757 Doctoral Dissertation, The Ohio State University, Columbus, OH,
758 2015.

759 (33) Zhang, Z.; Yao, J. G.; Boot-Handford, M. E.; Fennell, P.
760 Pressurised chemical-looping combustion of an iron-based oxygen
761 carrier: Reduction kinetic measurements and modelling. *Fuel Process.*
762 *Technol.* **2018**, *171*, 205–214.

763 (34) Goellner, J.; Shah, V.; Turner, M. J.; Kuehn, N. J.; Littlefield, J.;
764 Cooney, G.; Marriott, J. *Analysis of Natural Gas-to-Liquid Trans-*
765 *portation Fuels via Fischer-Tropsch*; National Energy Technology
766 Laboratory (NETL), U.S. Department of Energy (DOE): Pittsburgh,
767 PA, 2013; DOE/NETL-2013/1597.

768 (35) Luo, S.; Zeng, L.; Fan, L.-S. Chemical looping technology:
769 Oxygen carrier characteristics. *Annu. Rev. Chem. Biomol. Eng.* **2015**, *6*
770 (6), 53–75.

771 (36) Kathe, M., Xu, D., Hsieh, T., Simpson, J., Statnick, R., Tong, A.,
772 Fan, L.-S. *Chemical Looping Gasification for Hydrogen Enhanced Syngas*
773 *Production with In-Situ CO₂ Capture*; U.S. Department of Energy
774 (DOE): Washington, D.C., 2015; FE0012136, DOI: [DOI: 10.2172/1185194](https://doi.org/10.2172/1185194).

775 (37) Tong, A.; Sridhar, D.; Sun, Z.; Kim, H. R.; Zeng, L.; Wang, F.;
776 Wang, D.; Kathe, M.; Luo, S.; Sun, Y.; Fan, L.-S. Continuous high
777 purity hydrogen generation from a syngas chemical looping 25 kW_{th}
778 sub-pilot unit with 100% carbon capture. *Fuel* **2013**, *103* (103), 495–
779 505.

780 (38) Sridhar, D.; Tong, A.; Kim, H. R.; Zeng, L.; Li, F.; Fan, L.-S.
781 Syngas chemical looping process: Design and construction of a 25
782 kW_{th} subpilot unit. *Energy Fuels* **2012**, *26* (4), 2292–2302.